frontiers | Frontiers in Chemistry

TYPE Original Research
PUBLISHED 14 March 2023
DOI 10.3389/fchem.2023.1125835

OPEN ACCESS

EDITED BY
Sethumathavan Vadivel,
Tokyo Institute of Technology, Japan

REVIEWED BY
Abi Taddesse,
Haramaya University, Ethiopia
Yassine Slimani,
Imam Abdulrahman Bin Faisal University, Saudi Arabia

*CORRESPONDENCE
Mohamed Shaker S. Adam,
madam@kfu.edu.sa
Shahid Iqbal,
aat40292@gmail.com

SPECIALTY SECTION
This article was submitted to Photocatalysis and Photochemistry, a section of the journal Frontiers in Chemistry

RECEIVED 16 December 2022
ACCEPTED 23 February 2023
PUBLISHED 14 March 2023

CITATION
Adam MSS, Sikander S, Qamar MT, Iqbal S, Khalil A, Taha AM, Abdel-Rahman OS and Elkaeed EB (2023), Photocatalytic removal of imidacloprid containing frequently applied insecticide in agriculture industry using Co_3O_4 modified MoO_3 composites.
Front. Chem. 11:1125835.
doi: 10.3389/fchem.2023.1125835

Photocatalytic removal of imidacloprid containing frequently applied insecticide in agriculture industry using Co_3O_4 modified MoO_3 composites

Mohamed Shaker S. Adam[1,2]*, Sumbleen Sikander[3], M. Tariq Qamar[3], Shahid Iqbal[4]*, Ahmed Khalil[1,5], Amel Musa Taha[1], Obadah S. Abdel-Rahman[1] and Eslam B. Elkaeed[6]

[1]Department of Chemistry, College of Science, King Faisal University, Al-Ahsa, Saudi Arabia, [2]Department of Chemistry, Faculty of Science, Sohag University, Sohag, Egypt, [3]Department of Chemistry, Forman Christian College (A Chartered University), Lahore, Pakistan, [4]Department of Chemistry, School of Natural Sciences (SNS), National University of Science and Technology (NUST), Islamabad, Pakistan, [5]Chemistry Department, Faculty of Science, Zagazig University, Zagazig, Egypt, [6]Department of Pharmaceutical Sciences, College of Pharmacy, AlMaarefa University, Riyadh, Saudi Arabia

Water pollution caused by the frequent utilization of pesticides in the agriculture industry is one of the major environmental concerns that require proper attention. In this context, the photocatalytic removal of pesticides from contaminated water in the presence of metallic oxide photocatalysts is quite in approach. In the present study, Orthorhombic MoO_3 has been modified with varying amount of cobalt oxide through wet impregnation for the removal of imidacloprid and imidacloprid-containing commercially available insecticide. The solid-state absorption response and band gap evaluation of synthesized composites revealed a significant extension of absorption cross-section and absorption edge in the visible region of the light spectrum than pristine MoO_3. The indirect band gap energy varied from ~2.88 eV (MoO_3) to ~2.15 eV (10% Co_3O_4-MoO_3). The role of Co_3O_4 in minimizing the photo-excitons' recombination in MoO_3 was studied using photoluminescence spectroscopy. The orthorhombic shape of MoO_3 was confirmed through X-ray diffraction analysis and scanning electron microscopy. Moreover, the presence of distinct absorption edges and diffraction peaks corresponding to Co_3O_4 and MoO_3 in absorption spectra and XRD patterns, respectively verified the composite nature of 10% Co_3O_4-MoO_3. The photocatalytic study under natural sunlight irradiation showed higher photocatalytic removal (~98%) of imidacloprid with relatively higher rate by 10% Co_3O_4-MoO_3 composite among all contestants. Furthermore, the photocatalytic removal (~93%) of commercially applied insecticide, i.e., Greeda was also explored.

KEYWORDS

insecticide, imidacloprid, greeda, MoO3 composites, photocatalysis

Introduction

With the arrival of the Green Revolution in the 20th century, farmers started to use pesticides, insecticides, and herbicides to get higher yields. These chemicals are frequently applied by farmers not only in crops and farms but also in backyard gardens to prevent the agriculture field from the pest attack. The use of pesticides and insecticides at various stages has significantly increased food production and made food storage safer (Foster et al., 1991; Mateo-Sagasta et al., 2017). However, the excessive use of these toxins causes many adverse effects such as pollution of brooks, rivers, marshy areas, lakes, and also valleys, as these toxic manufactured chemicals run off into the nearby water streams which ultimately leads to the scarcity of clean water (Kaur et al., 2019). It is reported that the world is utilizing approximately 2.5 million tons of pesticides on an annual basis wherein very small quantities reach the target while the rest disperse through air, soil, and water which consequently leads to pollution (Hodgson and Levi, 1996).

Many concerns are shown by researchers nowadays because of the permanent existence of pesticides and insecticides in water and food as they also have inauspicious effects on human health and the equilibrium of the ecosystem (Carvalho, 2017; de Souza et al., 2020). Human health is badly affected by these toxins in the drinking water. These toxins have critical effects on mortals such as carcinogenesis, neurotoxicity effects on reproduction, and cell development effects, commonly in the early stages of life (Villaverde et al., 2017; Liang et al., 2019). Their effects are equally harmful to human beings, animals, and marine life. The situation is much critical in countries where water resources are limited, and lives are restricted to utilize contaminated water for various purposes. Therefore, it is an acute need to come up with an efficient and cost-effective technology for the removal of these toxins from contaminated water (Ahmed et al., 2011; Khan et al., 2015a).

Several water decontamination techniques have been utilized to remove the pollutants from the contaminated water such as adsorption, filtration, chemical oxidation, and biological treatments. In addition, many studies are available for the utilization of advanced oxidation methodologies such as photocatalytic process, heterogeneous catalytic oxidation with H_2O_2, Fenton/photo-Fenton oxidation, ozonation, and UV/H_2O_2 treatment for water purification (Swaminathan et al., 2013; Cardoso et al., 2021). Among these, heterogeneous photocatalysis for the complete removal and mineralization of organic toxins is becoming advantageous over others due to its reusability, recovery of photocatalysts, suitability, and sustainability (Qamar et al., 2017; Alhogbi et al., 2020; Aslam et al., 2022). Moreover, it is considered as a green process because natural sunlight can be used to initiate a photocatalytic process while generating reactive oxygen species (ROS) which ultimately leads to the conversion of pollutants into benign species (Zangeneh et al., 2015; Charanpahari et al., 2019).

The progress of photocatalysis is significantly based on the choice of a photocatalyst. In this context, metal oxides and metal oxide-based photocatalysts are being studied extensively for the removal of toxins due to their tunable morphological, structural, optical and photocatalytic properties (Mathiarasu et al., 2021; Hannachi et al., 2022a; Maqbool et al., 2022). Recently, ternary composite of MoO_3 with CuO, MoO_3/ZnO heterostructures, CuO/MoO_3 heterojunction, ZnO co-doped with Ce and Yb and MoO_3/g-C_3N_4 have been used as photocatalysts wherein a synergic effect of the components in a composite was considered responsible for the enhanced photocatalytic removal of organic dyes (Xue et al., 2019; Ramesh and Shivanna, 2021; Hannachi et al., 2022b; Hussain et al., 2022). In addition, many investigations related to the photocatalytic activities of TiO_2, ZnO, Fe_2O_3, WO_3, Bi_2O_3, V_2O_5, Cu_2O, NiO, *etc.*, Have also been reported (Khan et al., 2015b; Mathiarasu et al., 2021; Velempini et al., 2021; Hannachi et al., 2022a; Maqbool et al., 2022). However, the quest to investigate the potential contestant for the effective removal of toxic pollutants from the wastewater has not over yet and researchers are also paying attention to study the photocatalytic removal of pesticides and insecticides from the aqueous system in the illumination of light.

For the above-mentioned purpose, Molybdenum trioxide (MoO_3), an n-type semiconductor, can be an interesting candidate because of having wide band gap energy, ionic conductivity as a result of oxygen vacancies, layered structure, tunable optoelectronic properties and photocatalytic activity (Ijeh et al., 2020; Ali and Ahmad, 2022). Due to its enthralling electrical and optical properties, it is being used in various applications such as gas sensing, LED, smart windows, supercapacitors, batteries, energy storage, DSSCs, optical switch coatings and photocatalysis (Al-Muntaser et al., 2022; Noby et al., 2022; Selvakumar and Palanivel, 2022). However, its wide application in photocatalytic removal of organic toxins is limited due to its large band gap (~3.1 eV), smaller visible-light absorption cross-section and lower photo-excitons separation (Zheng et al., 2021).

In the above contexts, this study has been designed to address the two issues; Firstly, orthorhombic MoO_3 has been modified with Co_3O_4 through the wet-impregnation method to come up with a photocatalyst having larger light absorption spectrum, lower band gap energy and greater charge separation and transferability. Secondly, the successful removal of 15 ppm imidacloprid and imidacloprid containing commercially applied insecticide (Greeda) in the agriculture field under the exposure of natural sunlight. The reason for the utilization of Co_3O_4 to modify n-type MoO_3 is due to its light absorption capacity, narrow band

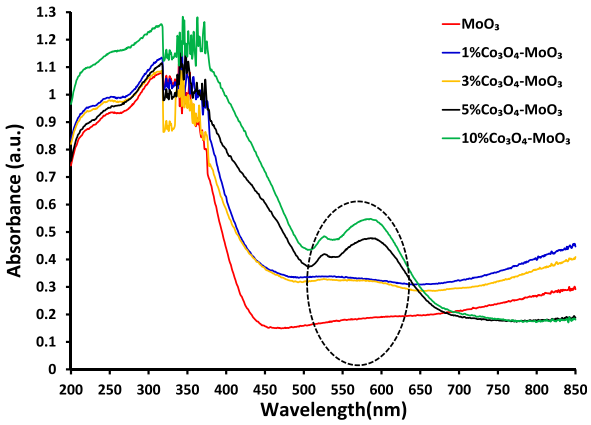

FIGURE 1
The comparison of solid-state absorption spectra of pristine and modified MoO_3.

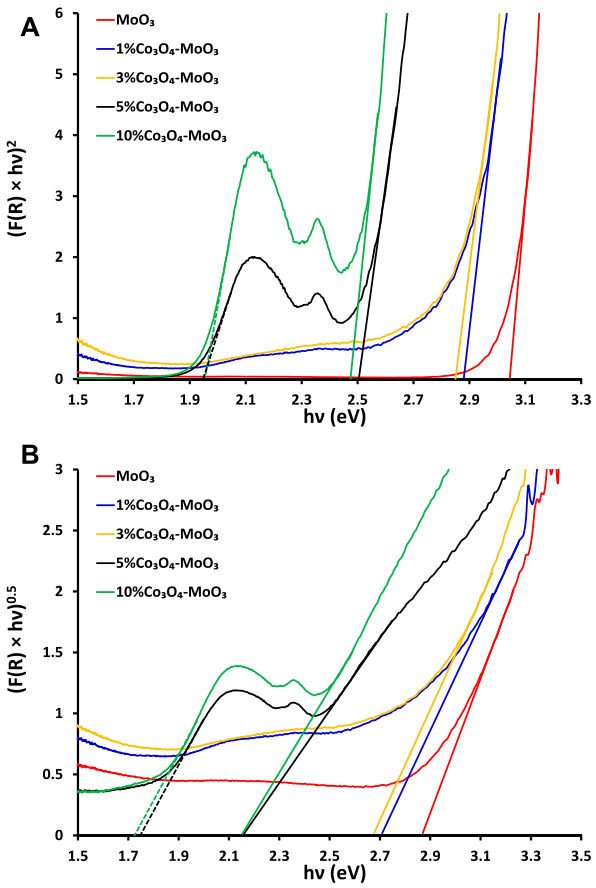

FIGURE 2
The graphical evaluation of **(A)** direct **(B)** indirect band gaps of pristine and modified MoO_3.

gap, good charge transportability and p-type semiconducting nature (Cao et al., 2022; Wang et al., 2023). Moreover, the successful contribution of Co_3O_4 in enhancing the photocatalytic activity of CeO_2, g-C_3N_4, TiO_2, Bi_2O_3 and Fe_2O_3 while generating photo-excitons' separation is well established (Ranjith et al., 2019; Niu et al., 2022; Reena et al., 2022). Previously, rare studies are available for the removal of imidacloprid over MoO_3-based photocatalysts (Adabavazeh et al., 2021; Zhang et al., 2021). However, there is no investigation is present yet for the removal of imidacloprid and Greeda over Co_3O_4-modified orthorhombic MoO_3 under the illumination of natural sunlight.

Experimental

Orthorhombic MoO_3 was prepared using co-precipitation method. In this context, 12.35 g $(NH_4)_6Mo7O24.4H2O$ (Sigma-Aldrich, ≥99%) was dissolved in distilled water with continuous stirring for an hour at room temperature. Then 2 mL Triton X-100 (Sigma-Aldrich, laboratory-grade) was added to the clear solution. The mixture was then acidified with slow addition of 0.1 M HNO_3 (Sigma-Aldrich, 70%) to attain the pH of the solution to 2 with constant heating at 50°C till the formation of precipitates. The precipitates were separated from the mixture through filtration, washed, and dried in an oven at 100°C. The dried precipitates were calcined at 500°C for 4 h at 10°C/min in a Vulcan D-550 muffle furnace. The calcined material was ground using mortar and pestle to get powder of α-MoO_3 photocatalyst.

The Co_3O_4-modified MoO_3 was synthesized using the wet-impregnation method (Scheme 1). The composite of 1 wt% Co_3O_4-MoO_3 was prepared by dissolving 0.15 g Co $(NO_3)_2.6H_2O$ (Sigma-Aldrich, ≥99%) in distilled water in a beaker (100 mL) with continuous stirring at room temperature. Then, 3.0 g pre-synthesized α-MoO_3 was added to the cobalt nitrate solution under continuous stirring at 80°C. The mixture was kept on a hot plate till complete dryness at 80°C. The dried material was collected and calcined at 500°C for 4 h at 10°C/min in a Vulcan D-550 muffle furnace. The calcined material was ground using mortar and pestle to get powder of 1 wt% Co_3O_4-MoO_3 photocatalyst. Moreover, a similar procedure was adopted to synthesize 3, 5, and 10 wt% Co_3O_4-MoO_3 by using 0.45, 0.75 and 1.5 g Co $(NO_3)_2.6H_2O$, respectively.

The synthesized materials were characterized using optical, structural and morphological techniques. The solid-state absorption spectra were recorded in the 200–850 nm range using Perkin Elmer UV-visible diffuse reflectance spectrophotometer whereas the band gap energy of the synthesized materials was

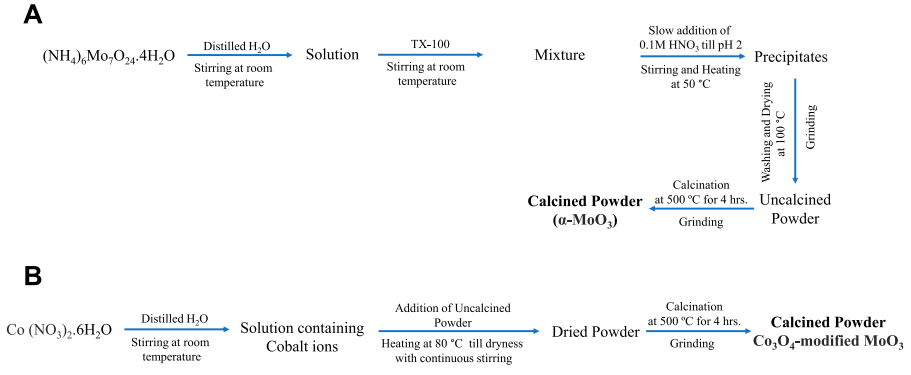

SCHEME 1
The schematic presentation for the synthesis of **(A)** α-MoO_3 and **(B)** Co_3O_4-modified MoO_3 powders.

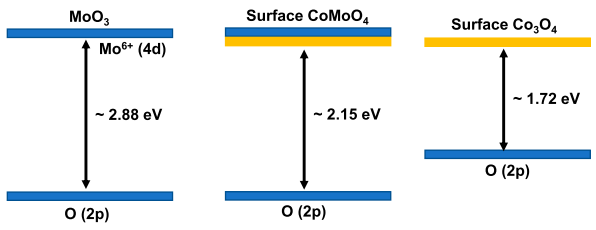

SCHEME 2
The representation of band gaps in synthesized materials.

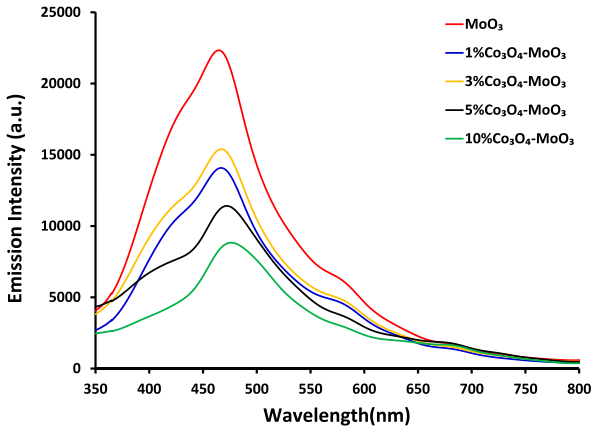

FIGURE 3
The comparison of photoluminescence spectra of pristine and modified MoO_3.

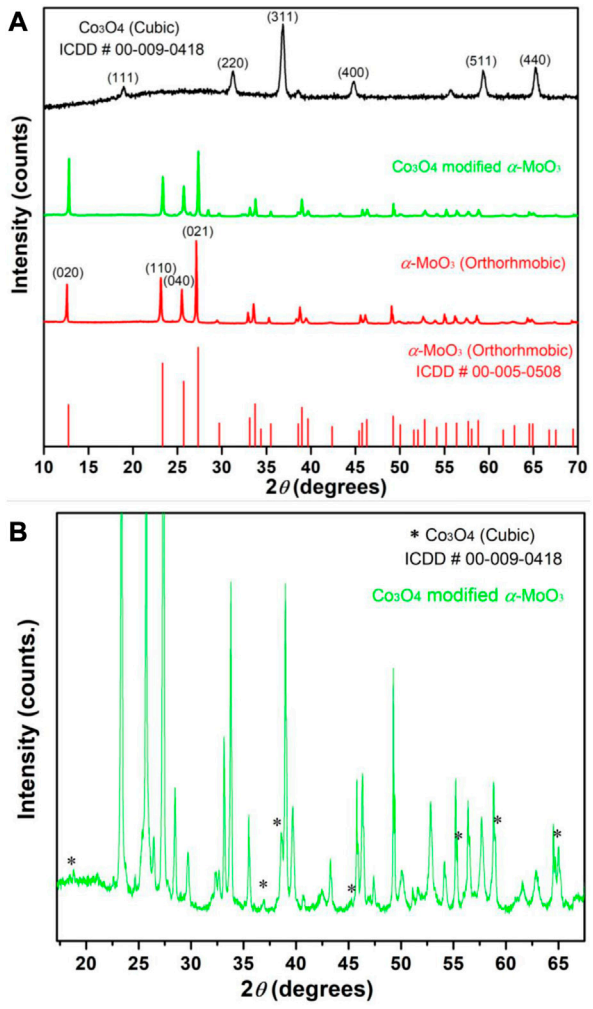

FIGURE 4
The XRD patterns of **(A)** α-MoO_3, Co_3O_4 and 10% Co_3O_4 modified MoO_3 whereas **(B)** is the exploded XRD pattern of 10% Co_3O_4 modified MoO_3 with clearly marked (*) reflections by Co_3O_4.

estimated using Kubelka- Munk, *F(R),* the transformation of reflectance (%). The change in photo-excitons recombination was noticed from the photoluminescence response of the materials acquired from fluorescence spectrometer, RF-5301 PC, Shimadzu, Japan, at 200 nm excitation wavelength. The XRD patterns were recorded from 5 to 90 with 0.02° step size by X'pert X-ray powder diffractometer (Philips PW1398) having Cu Kα radiation source. Moreover, the morphology of the 10% Co_3O_4-MoO_3 was examined by field-emission scanning electron microscopy (Hitachi, SU8010, Tokyo, Japan).

The photocatalytic removal of 15 ppm imidacloprid (Merck, Analytical standard) was studied under the illumination of natural sunlight (900 ± 50 × 10^2 lx). In a typical experiment, the optimized dose of pristine MoO_3 (150 mg) was suspended in 100 mL 15 ppm imidacloprid aqueous solution and stirred for 10 min. The suspension was poured into a glass reactor of 14 cm (diameter) and 2 cm (height) and kept in dark for 30 min. After 30 min, the glass reactor was exposed to natural sunlight. The samples were collected after a regular time interval (light exposure) of 30 min and filtered using a 0.20 µm syringe filter. The filtered samples were then subjected to a UV-visible spectrophotometer (UV-1800, Shimadzu, Japan) for the monitoring of imidacloprid removal while selecting its absorbance at a characteristic wavelength, i.e., 270 nm (λ_{max}) (Kanwal et al., 2018). The same procedure was adopted to monitor the removal of 15 ppm imidacloprid over other synthesized Co_3O_4-modified MoO_3 composites.

In order to study the removal of imidacloprid from the polluted water, the samples were collected using a syringe filter from the suspension exposed to the light after a regular interval and were subjected to UV-visible spectrophotometer for the determination of the concentration of removed pollutant which ultimately led to the % removal of imidacloprid by the photocatalyst under the exposure of light using the following equation (Garg et al., 2021).

$$\%\, removal = \frac{C_o - C_t}{C_o} \times 100 \quad (1)$$

Here, C_o is the pollutant initial concentration whereas C_t is the concentration of the pollutant after exposure time '*t*'. Moreover, the validity of Langmuir Hinshelwood (L-H) kinetic models was also studied using the following equation to evaluate the kinetics of

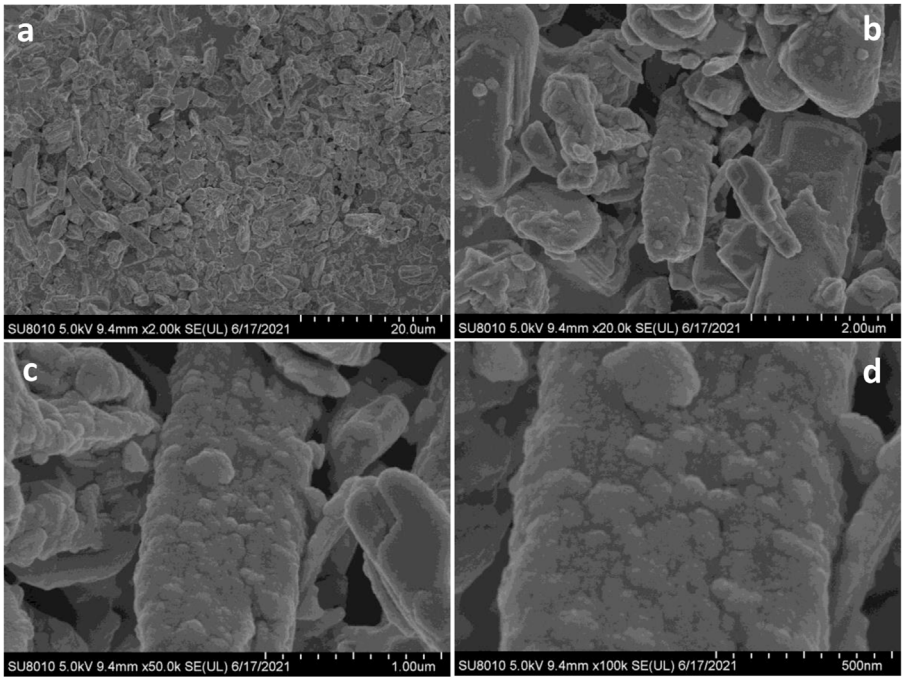

FIGURE 5
The scanning electron micrographs of 10% Co_3O_4-MoO_3 at **(A)** 2.0 k **(B)** 20.0 k **(C)** 50.0 k and **(D)** 100 k magnifications.

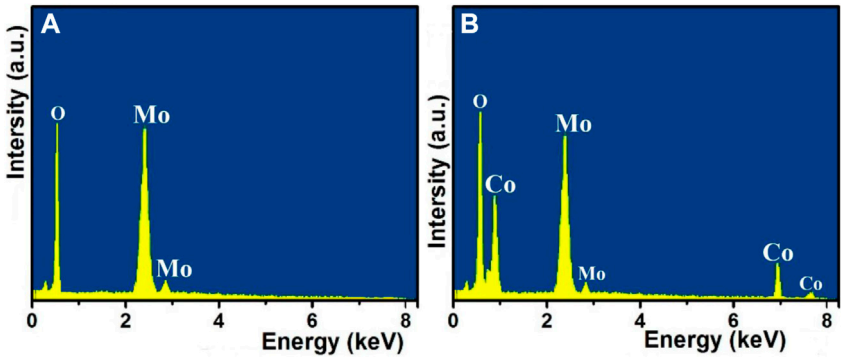

FIGURE 6
The EDX spectra of **(A)** pure MoO_3 and **(B)** 10% Co_3O_4-MoO_3.

photocatalytic removal of organic pollutants under the exposure of light (Alhogbi et al., 2020).

$$ln \frac{C_o}{C_t} = k \times t \quad (2)$$

Here, k is the rate constant which was determined from the slope by plotting $ln \frac{C_o}{C_t}$ V t.

Moreover, the photocatalytic removal of 15 ppm Greeda (Agricom international, Jiangsu Pesticide Research Institute, Jiangsu, China), a commercially available insecticide in the agriculture field, over 10% Co_3O_4-MoO_3 was also investigated under the illumination of natural sunlight.

Results and discussion

The comparison of solid-state absorption spectra of MoO3 and its composites is presented in Figure 1 Which indicates the beneficial role of Co3O4 in increasing the absorption cross-section of MoO3. Wherein, maximum effect

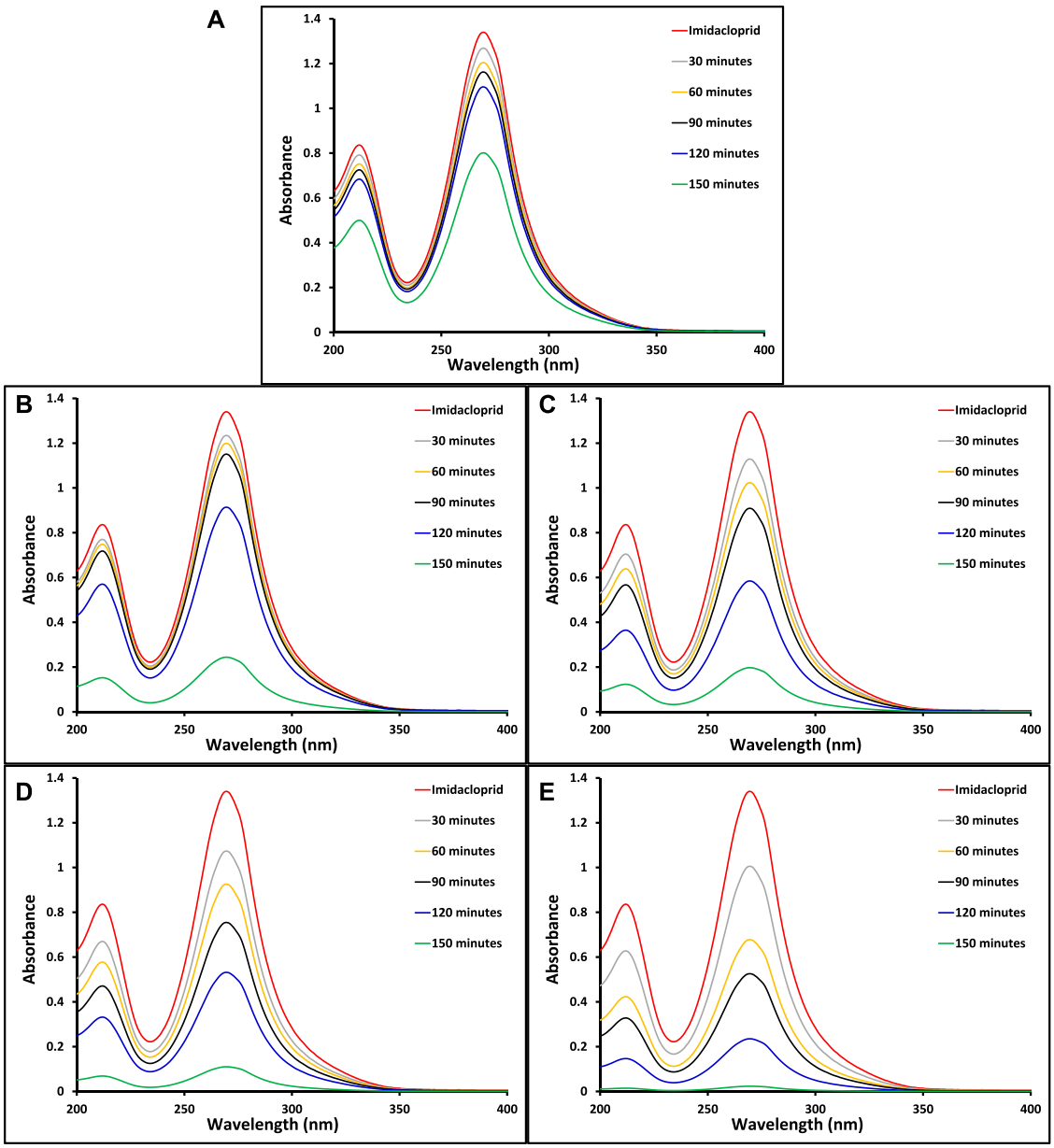

FIGURE 7
The comparison of absorption spectra for the removal of imidacloprid by **(A)** pristine MoO_3 **(B)** 1% Co_3O_4-MoO_3 **(C)** 3% Co_3O_4-MoO_3 **(D)** 5% Co_3O_4-MoO_3 and **(E)** 10% Co_3O_4-MoO_3 at different light exposure time.

in enhancing the absorption response was noticed for 10% Co3O4-MoO3 composite. Moreover, the presence of distinct absorption due to Co3O4 (encircled in Figure 1) in addition to the major absorption corresponding to MoO3 confirms the composite nature of the synthesized materials. Band gap energy of the synthesized materials has been estimated by plotting $(F(R) \times h\nu)^{1/n}$ *versus* hυ (eV). Here, "n" can be ½ or two which corresponds to direct or indirect band gaps evaluation, respectively and F(R) is Kubelka–Munk function. The direct and indirect band gap evaluations (Figures 2A,B) reveal a lowering in the band gap energy of composite materials as compared to pristine MoO_3. The evaluated indirect band gap (~2.88 eV), as shown in Figure 2B has close agreement with literature values for MoO_3 which is mainly due to the excitations of the electron from O (2p) to Mo (4days) (Qamar et al., 2017). Whereas, the decrease in band gap energy of the composite than pristine MoO_3 is attributed to the introduction of cobalt (3days-4s) orbitals below in the vicinity of the MoO_3 conduction band as shown in Scheme 2. The indirect band gap energies, estimated by extrapolating $(F(R) \times h\nu)^{0.5}$ vs. $h\nu$ curves to the horizontal axis were ~2.70 eV, ~2.68 eV, ~2.16 eV and ~2.15 eV for 1%, 3%, 5% and 10% Co_3O_4-MoO_3, respectively as shown in Figure 2B. The

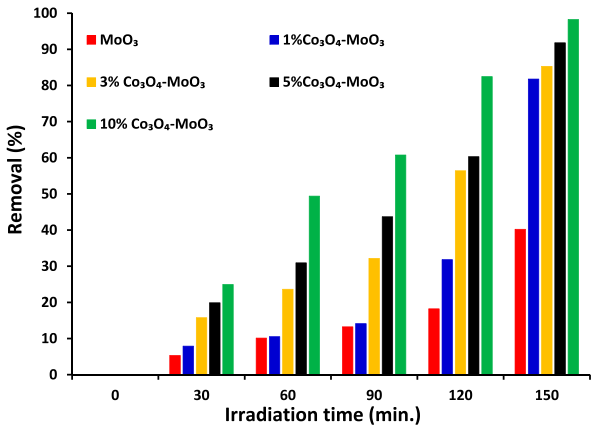

FIGURE 8
The comparison of removal (%) of 15 ppm imidacloprid by α-MoO_3 and its composite with Co_3O_4 under the illumination of natural sunlight (800 ± 50 × 10^2 lx) at different light exposures' duration.

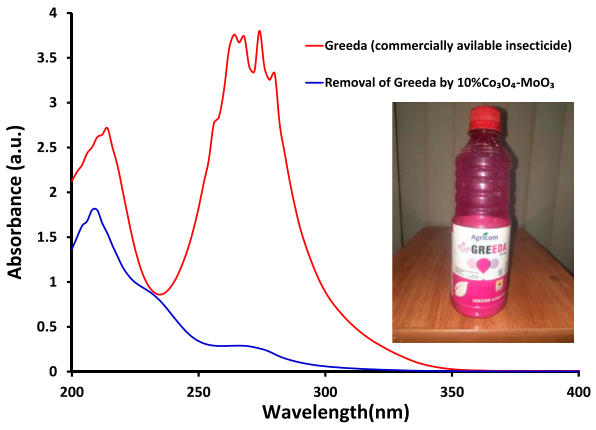

FIGURE 10
The comparison of absorption spectra of Greeda, a commercially available insecticide, (red) initially taken and (blue) after 150 min of light exposure in the presence of 10% Co_3O_4-MoO_3 photocatalyst.

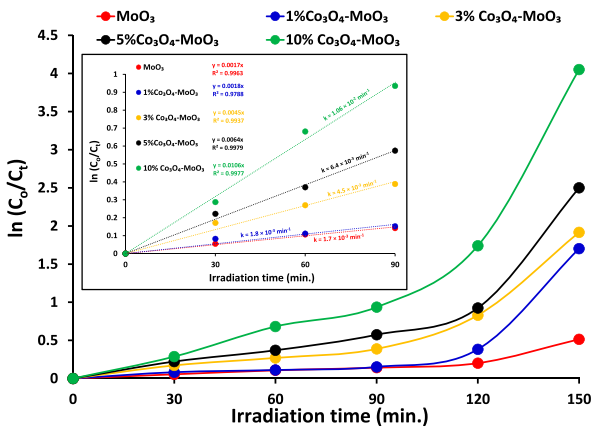

FIGURE 9
The comparison of rate of removal of imidacloprid (15 ppm) by α-MoO_3 and its composite with Co_3O_4 under the illumination of natural sunlight (800 ± 50 × 10^2 lx). Whereas, inset shows the estimation of rate constants.

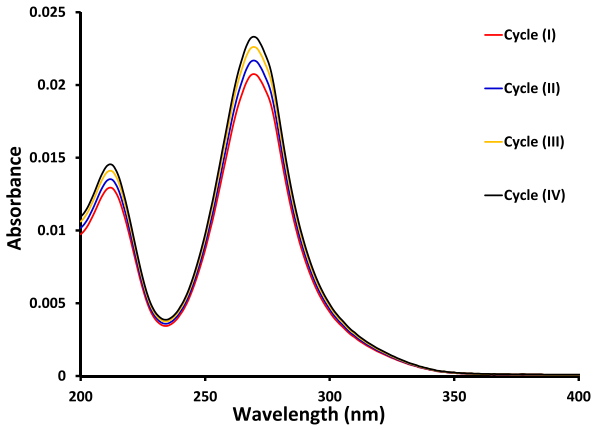

FIGURE 11
The comparison of absorption spectra for the removal of imidacloprid by 10% Co_3O_4-MoO_3 photocatalyst in exposure of natural sunlight for 150 min in four cycles at an interval of 24 h.

prominent multiple band edge near ~1.7 eV was also noticed at higher loading (5% and 10%) of Co_3O_4 in composites, which is in accordance with band gap energy of Co_3O_4 presented in literature (Bhargava et al., 2018; Anuradha and Raji, 2020). Hence, the presence of these multiple edges in modified MoO_3 confirms the composite nature of the synthesized photocatalyst.

Figure 3 depicts the comparison of photoluminescence spectra of synthesized photocatalysts, where a successive decrease in emission intensity was noticed for all composites as compared to pristine MoO_3 indicating the supporting role of Co_3O_4 in lowering the recombination process. Among composites, 10% Co_3O_4-MoO_3 showed the smallest photo-excitons (e-–h+) recombination which favors the fruitful use of photo-excitons in photocatalytic removal of target pollutant, i.e., insecticide. Moreover, a ~60% decrease in emission intensity was observed for 10% Co_3O_4-MoO_3 whereas ~31, ~3 seven and ~49% decrease in emission intensity was noticed for 1, 3, and 5% Co_3O_4-MoO_3 composites, respectively.

The comparison of x-ray diffraction patterns of the synthesized MoO_3, Co_3O_4 and 10% Co_3O_4 modified MoO_3 is presented in Figure 4. An orthorhombic phase of the synthesized α-MoO_3 with lattice parameters (a = 3.9620 Å, b = 13.8580 Å, c = 3.6970 Å and α = β = γ = 90°) and cubic phase of Co_3O_4 having lattice parameters (a = b = c = 8.0840 Å and α = β = γ = 90°) was confirmed by matching diffractions patterns with ICDD# 00–006-0508 and 00–009-0418, respectively as shown in Figure 4A. The XRD pattern of 10% Co_3O_4 modified MoO_3 in Figure 4A, clearly shows the dominancy of diffraction peaks arising due to the MoO_3 as compared to the additional peaks due to the presence of cubic Co_3O_4 which have been marked by (*) in Figure 4B.

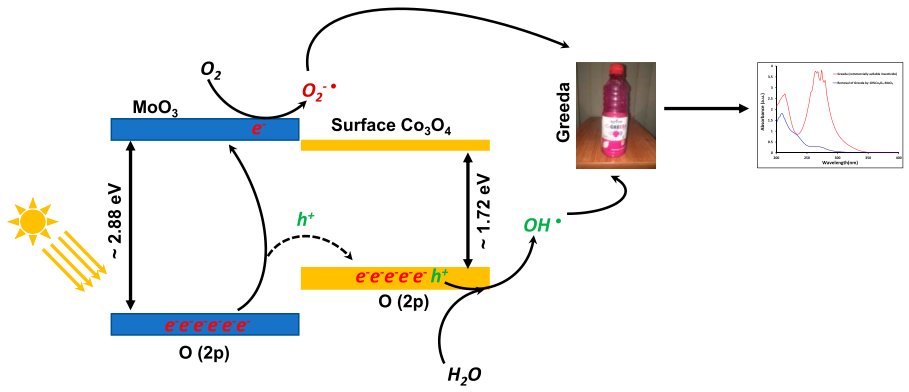

SCHEME 3
The schematic representation for the absorption of photon, photo-excitons' separation and the removal of Greeda in the exposure of natural sunlight.

The presence of additional peaks due to cubic Co_3O_4 in the XRD pattern of orthorhombic MoO_3 confirms the composite nature of the newly synthesized photocatalysts. In addition to the presence of cubic Co_3O_4 (ICDD# 00–009-0418) as the major phase in α-MoO_3, a couple of low-intensity reflections also specified the occurrence of monoclinic $CoMoO_4$ (ICDD# 00–021-0868). The existence of $CoMoO_4$ may be attributed to the attachment of Cobalt with the surface oxygen shared by Mo. The average crystallite sizes of the pristine MoO_3 and 10% Co_3O_4 modified MoO_3 were calculated using reflections at 2θ values of 12.68°, 23.27°, 25.87° and 27.25° with the help of the Debye–Scherrer equation. Wherein a mild increase in crystallite size for the composite sample was noticed as compared to pure MoO_3. The estimated average crystallite sizes of α-MoO_3, 10% Co_3O_4-MoO_3 and Co_3O_4 powders were ~54.42 nm, ~58.43 nm and ~20.63 nm, respectively. Average crystallite size of Co_3O_4 powder was evaluated using reflections at 2θ values of 31.25°, 36.84° and 65.22°.

Moreover, the morphology of 10% Co_3O_4-MoO_3 was also explored at different magnification as shown in Figure 5 wherein the presence of Co_3O_4 were noticed on the surface of orthorhombic MoO_3. The orthorhombic morphology of MoO_3 was in accordance with XRD diffraction pattern of MoO_3 (ICDD# 00–021-0868). The observed homogeneous distribution of Co_3O_4 on the surface of MoO_3 verifies the composite form of the synthesized photocatalysts and the distributed Co_3O_4 played a significant role in enhancing the absorption of light and then increasing the photocatalytic efficiency of α- MoO_3 in natural sunlight.

Energy-dispersive X-ray spectroscopy was used to further determine the composition and element distribution of the MoO_3 that had been synthesized in its as-prepared state (Figure 6A) and the 10% Co_3O_4-MoO_3 (Figure 6B). According to the findings, which are displayed in Figure 6B, the 10% Co_3O_4-MoO_3 composites displayed a spatial distribution of O, Mo, and Co species. The high intensity of the detection of O, Mo, and Co showed that each element was spread out evenly in the 10% Co_3O_4-MoO_3 composites.

The ultimate goal of this study was to investigate the removal of imidacloprid and Greeda under the illumination of natural sunlight. Before the exposure of suspension containing photocatalyst and imidacloprid to light as mentioned in the experimental section, the suspension was kept in dark for 30 min to establish an equilibrium between pollutant and catalyst. The photolysis of imidacloprid was also evaluated by recording the absorption spectrum of the substrate after 150 min of light exposure without the presence of a photocatalyst. The amount of photocatalyst was also optimized (150 mg of photocatalyst) while studying the photocatalytic removal of 15 ppm imidacloprid with varying doses of MoO_3 catalyst under the illumination of natural sunlight. The comparison of absorption spectra of imidacloprid's removal over pristine and modified MoO_3 under the illumination of sunlight (800 ± 50 × 102 lx) is provided in Figure 7 at different exposure times. Moreover, higher photodegradation (~98%) was noticed for 10% Co3O4-MoO3 followed by 5% Co_3O_4-MoO_3 (~92%), 3% Co_3O_4-MoO_3 (~85%) and 1% Co_3O_4-MoO_3 (~81%) and MoO_3 (~41%) after 150 min of sunlight exposure. As shown in Figure 8 The decreasing trend of removal efficiency (%) of the photocatalysts is given below.

10 % Co_3O_4-MoO_3 > 5 % Co_3O_4-MoO_3 > 3 % Co_3O_4-MoO_3 > 1 % Co_3O_4-MoO_3 > MoO_3

The kinetic study reveals that the photocatalytic removal of imidacloprid by newly synthesized materials did not follow the Langmuir Hinshelwood (L-H) kinetic model throughout light exposure from 0 to 150 min as shown in Figure 9. However, in the initial 90 min the rate of removal followed Langmuir Hinshelwood (L-H) kinetic model and the estimated rate constants are 1.7×10^{-3} min^{-1}, 1.8×10^{-3} min^{-1}, 4.5×10^{-3} min^{-1}, 6.4×10^{-3} min^{-1} and 1.1×10^{-2} min^{-1} by MoO_3, 1% Co_3O_4-MoO_3, 3% Co_3O_4-MoO_3, 5% Co_3O_4-MoO_3 and 10% Co_3O_4-MoO_3, respectively as provided in the inset of Figure 9. The higher removal efficiency of Co_3O_4-MoO_3 as compared to pristine MoO_3 may be attributed to the synergic role of Co_3O_4 in increasing the life span of photo-excitons by lowering the charge recombination process (Figure 3), which ultimately leads to the higher removal of imidacloprid. In order to assess the application of an efficient photocatalyst declared in this study, i.e., 10% Co_3O_4-MoO_3 for the removal of insecticide, Greeda (a commercially available frequently applied insecticide in the agriculture field) was chosen. Figure 10 shows that ~93% of Greeda was removed by 10% Co_3O_4-MoO_3 in 150 min of

natural sunlight exposure. Previously, the photocatalytic removal of imidacloprid was explored previously using iron-based catalysts, ZnO, TiO_2, SnO_2 ternary nanocomposites, g-C_3N_4 and WO_3 under the exposure of UV and visible light, however, studies pertaining to the removal of Greeda and Imidacloprid using Co_3O_4-MoO_3 photocatalysts are not evident from the literature. (Guzsvány et al., 2010; Derbalah et al., 2019; Yari et al., 2019; Sudhaik et al., 2020; Li et al., 2022; Faisal et al., 2023). The efficiency of 10% Co_3O_4-MoO_3 photocatalyst after four cycles was also investigated and a minor decrease in efficiency was noticed for the removal of imidacloprid as shown in Figure 11. Moreover, the mechanism for the removal of Greeda in the exposure of natural sunlight by Co_3O_4 modified MoO_3 composite is provided in Scheme 3.

Conclusion

The successful synthesis of Co_3O_4-modified MoO_3 composites through the wet-impregnation method and their photocatalytic activities lead to the following conclusions.

- The successfully distributed Co_3O_4 on the surface of orthorhombic MoO_3 played a significant role in improving the spectral response and lowering the bandgap energy of α- MoO_3 from ~2.88 eV to ~2.15 eV.
- The higher e^-–h^+ recombination in α- MoO_3 was successfully suppressed by modifying MoO_3 with Co_3O_4.
- All modified MoO_3 photocatalysts presented higher photocatalytic activity for the removal of imidacloprid under the illumination of natural sunlight due to the synergic effect of Co_3O_4.
- A commercially available insecticide (Greeda) was successfully removed (~93%) by 10% Co_3O_4-MoO_3 in 150 min of natural sunlight exposure.

Data availability statement

The original contributions presented in the study are included in the article/supplementary material, further inquiries can be directed to the corresponding authors.

Author contributions

The manuscript was written with the contributions of all authors. All authors have approved the final version of the manuscript.

Acknowledgments

The authors extend their appreciation to the Deputyship for Research and Innovation, Ministry of Education in Saudi Arabia for funding this research work (project number INST060).

Conflict of interest

The authors declare that the research was conducted in the absence of any commercial or financial relationships that could be construed as a potential conflict of interest.

Publisher's note

All claims expressed in this article are solely those of the authors and do not necessarily represent those of their affiliated organizations, or those of the publisher, the editors and the reviewers. Any product that may be evaluated in this article, or claim that may be made by its manufacturer, is not guaranteed or endorsed by the publisher.

References

Adabavazeh, H., Saljooqi, A., Shamspur, T., and Mostafavi, A. (2021). Synthesis of polyaniline decorated with ZnO and $CoMoO_4$ nanoparticles for enhanced photocatalytic degradation of imidacloprid pesticide under visible light. *Polyhedron* 198, 115058. doi:10.1016/j.poly.2021.115058

Ahmed, A., Randhawa, M. A., Yusuf, M. J., and Khalid, N. (2011). Effect of processing on pesticide residues in food crops: A review. *Journal of Agricultural Research* 49 (3), 379–390.

Al-Muntaser, A., Pashameah, R. A., Sharma, K., Alzahrani, E., Farea, M., and Morsi, M. (2022). α-MoO_3 nanobelts/CMC-PVA nanocomposites: Hybrid materials for optoelectronic and dielectric applications. *J. Polym. Res.* 29 (7), 274–311. doi:10.1007/s10965-022-03134-y

Alhogbi, B. G., Aslam, M., Hameed, A., and Qamar, M. T. (2020). The efficacy of Co_3O_4 loaded WO3 sheets for the enhanced photocatalytic removal of 2, 4, 6-trichlorophenol in natural sunlight exposure. *J. Hazard. Mater.* 397, 122835. doi:10.1016/j.jhazmat.2020.122835

Ali, S. A., and Ahmad, T. (2022). Chemical strategies in molybdenum based chalcogenides nanostructures for photocatalysis. *Int. J. Hydrogen Energy* 47, 29255–29283. doi:10.1016/j.ijhydene.2022.06.269

Anuradha, C., and Raji, P. (2020). Facile synthesis and characterization of Co_3O_4 nanoparticles for high-performance supercapacitors using Camellia sinensis. *Appl. Phys. A* 126 (3), 164–212. doi:10.1007/s00339-020-3352-8

Aslam, M., Qamar, M. T., Soomro, M. T., Danish, E. Y., Ismail, I. M., and Hameed, A. (2022). The role of size-controlled CeO_2 nanoparticles in enhancing the stability and photocatalytic performance of ZnO in natural sunlight exposure. *Chemosphere* 289, 133092. doi:10.1016/j.chemosphere.2021.133092

Bhargava, R., Khan, S., Ahmad, N., and Ansari, M. M. N. (2018). "Investigation of structural, optical and electrical properties of Co_3O_4 nanoparticles," in AIP conference proceedings, Melville, New York, 08 May 2018 (AIP Publishing LLC), 030034.1953

Cao, Q., Li, Q., Pi, Z., Zhang, J., Sun, L.-W., Xu, J., et al. (2022). Metal–organic-framework-derived ball-flower-like porous Co3O4/Fe2O3 heterostructure with enhanced visible-light-driven photocatalytic activity. *Nanomaterials* 12 (6), 904. doi:10.3390/nano12060904

Cardoso, I. M., Cardoso, R. M., and da Silva, J. C. E. (2021). Advanced oxidation processes coupled with nanomaterials for water treatment. *Nanomaterials* 11 (8), 2045. doi:10.3390/nano11082045

Carvalho, F. P. (2017). Pesticides, environment, and food safety. *Food energy Secur.* 6 (2), 48–60. doi:10.1002/fes3.108

Charanpahari, A., Gupta, N., Devthade, V., Ghugal, S., and Bhatt, J. (2019). Ecofriendly nanomaterials for sustainable photocatalytic decontamination of organics and bacteria. *Handb. Ecomater.* 3, 1777–1805. doi:10.1007/978-3-319-48281-1_179-1

de Souza, R. M., Seibert, D., Quesada, H. B., de Jesus Bassetti, F., Fagundes-Klen, M. R., and Bergamasco, R. O. (2020). Occurrence, impacts and general aspects of pesticides in surface water: A review. *Process Saf. Environ. Prot.* 135, 22–37. doi:10.1016/j.psep.2019.12.035

Derbalah, A., Sunday, M., Chidya, R., Jadoon, W., and Sakugawa, H. (2019). Kinetics of photocatalytic removal of imidacloprid from water by advanced oxidation processes with respect to nanotechnology. *J. Water Health* 17 (2), 254–265. doi:10.2166/wh.2019.259

Faisal, M., Ahmed, J., Algethami, J. S., Jalalah, M., Alsareii, S. A., Alsaiari, M., et al. (2023). Visible-light responsive Au nanoparticle-decorated polypyrrole-carbon black/SnO_2 ternary nanocomposite for ultrafast removal of insecticide imidacloprid and methylene blue. *J. Industrial Eng. Chem.*, doi:10.1016/j.jiec.2023.01.032

Foster, S., Chilton, P., and Stuart, M. E. (1991). Mechanisms of groundwater pollution by pesticides. *Water Environ. J.* 5 (2), 186–193. doi:10.1111/j.1747-6593.1991.tb00606.x

Garg, R., Gupta, R., and Bansal, A. (2021). Photocatalytic degradation of imidacloprid using semiconductor hybrid nano-catalyst: Kinetics, surface reactions and degradation pathways. *Int. J. Environ. Sci. Technol.* 18 (6), 1425–1442. doi:10.1007/s13762-020-02866-y

Guzsvány, V., Banić, N., Papp, Z., Gaál, F., and Abramović, B. (2010). Comparison of different iron-based catalysts for photocatalytic removal of imidacloprid. *React. Kinet. Mech. Catal.* 99 (1), 225–233. doi:10.1007/s11144-009-0106-1

Hannachi, E., Slimani, Y., Nawaz, M., Sivakumar, R., Trabelsi, Z., Vignesh, R., et al. (2022). Preparation of cerium and yttrium doped ZnO nanoparticles and tracking their structural, optical, and photocatalytic performances. *J. Rare Earths*. doi:10.1016/j.jre.2022.03.020

Hannachi, E., Slimani, Y., Nawaz, M., Trabelsi, Z., Yasin, G., Bilal, M., et al. (2022). Synthesis, characterization, and evaluation of the photocatalytic properties of zinc oxide co-doped with lanthanides elements. *J. Phys. Chem. Solids* 170, 110910. doi:10.1016/j.jpcs.2022.110910

Hodgson, E., and Levi, P. E. (1996). Pesticides: An important but underused model for the environmental health sciences. *Environ. Health Perspect.* 104 (1), 97–106. doi:10.2307/3432700

Hussain, M. K., Khalid, N., Tanveer, M., Kebaili, I., and Alrobei, H. (2022). Fabrication of CuO/MoO_3 pn heterojunction for enhanced dyes degradation and hydrogen production from water splitting. *Int. J. Hydrogen Energy* 47 (34), 15491–15504. doi:10.1016/j.ijhydene.2021.11.090

Ijeh, R. O., Nwanya, A. C., Nkele, A. C., Madiba, I. G., Bashir, A., Ekwealor, A., et al. (2020). Optical, electrical and magnetic properties of copper doped electrodeposited MoO_3 thin films. *Ceram. Int.* 46 (8), 10820–10828. doi:10.1016/j.ceramint.2020.01.093

Kanwal, M., Tariq, S. R., and Chotana, G. A. (2018). Photocatalytic degradation of imidacloprid by Ag-ZnO composite. *Environ. Sci. Pollut. Res.* 25 (27), 27307–27320. doi:10.1007/s11356-018-2693-8

Kaur, R., Mavi, G. K., Raghav, S., and Khan, I. (2019). Pesticides classification and its impact on environment. *Int. J. Curr. Microbiol. Appl. Sci.* 8 (3), 1889–1897. doi:10.20546/ijcmas.2019.803.224

Khan, M. M., Adil, S. F., and Al-Mayouf, A. (2015). Metal oxides as photocatalysts. *Elsevier* 19, 462–464. doi:10.1016/j.jscs.2015.04.003

Khan, M., Mahmood, H. Z., and Damalas, C. A. (2015). Pesticide use and risk perceptions among farmers in the cotton belt of Punjab, Pakistan. *Crop Prot.* 67, 184–190. doi:10.1016/j.cropro.2014.10.013

Li, J., Chen, J., Ao, Y., Gao, X., Che, H., and Wang, P. (2022). Prominent dual Z-scheme mechanism on phase junction WO_3/CdS for enhanced visible-light-responsive photocatalytic performance on imidacloprid degradation. *Sep. Purif. Technol.* 281, 119863. doi:10.1016/j.seppur.2021.119863

Liang, L., Wang, Z., and Li, J. (2019). The effect of urbanization on environmental pollution in rapidly developing urban agglomerations. *J. Clean. Prod.* 237, 117649. doi:10.1016/j.jclepro.2019.117649

Maqbool, H., Bibi, I., Nazeer, Z., Majid, F., Ata, S., Raza, Q., et al. (2022). Effect of dopant on ferroelectric, dielectric and photocatalytic properties of Co–La-doped dysprosium chromite prepared via microemulsion route. *Ceram. Int.* 48 (21), 31763–31772. doi:10.1016/j.ceramint.2022.07.103

Mateo-Sagasta, J., Zadeh, S. M., Turral, H., and Burke, J. (2017). Water pollution from agriculture: A global review. *Exec. Summ.* 6 (5), 115–145.

Mathiarasu, R. R., Manikandan, A., Panneerselvam, K., George, M., Raja, K. K., Almessiere, M. A., et al. (2021). Photocatalytic degradation of reactive anionic dyes RB5, RR198 and RY145 via rare Earth element (REE) lanthanum substituted CaTiO3 perovskite catalysts. *J. Mater. Res. Technol.* 15, 5936–5947. doi:10.1016/j.jmrt.2021.11.047

Niu, B., Xiao, J., and Xu, Z. (2022). Recycling spent LiCoO2 battery as a high-efficient lithium-doped graphitic carbon nitride/Co3O4 composite photocatalyst and its synergistic photocatalytic mechanism. *Energy and Environ. Mater.*, doi:10.1002/eem2.12312

Noby, S. Z., Mohanty, A., Zirak, P., Ramadoss, A., and Schmidt-Mende, L. (2022). Hierarchical carbon coated vertically aligned α-MoO_3 nanoblades anode materials for supercapacitor application. *J. Alloys Compd.* 918, 165530. doi:10.1016/j.jallcom.2022.165530

Qamar, M. T., Aslam, M., Rehan, Z., Soomro, M. T., Ahmad, I., Ishaq, M., et al. (2017). MoO_3 altered ZnO: A suitable choice for the photocatalytic removal of chloroacetic acids in natural sunlight exposure. *Chem. Eng. J.* 330, 322–336. doi:10.1016/j.cej.2017.07.168

Ramesh, A. M., and Shivanna, S. (2021). Hydrothermal synthesis of MoO_3/ZnO heterostructure with highly enhanced photocatalysis and their environmental interest. *J. Environ. Chem. Eng.* 9 (2), 105040. doi:10.1016/j.jece.2021.105040

Ranjith, R., Renganathan, V., Chen, S.-M., Selvan, N. S., and Rajam, P. S. (2019). Green synthesis of reduced graphene oxide supported TiO_2/Co_3O_4 nanocomposite for photocatalytic degradation of methylene blue and crystal violet. *Ceram. Int.* 45 (10), 12926–12933. doi:10.1016/j.ceramint.2019.03.219

Reena, R. S., Aslinjensipriya, A., Infantiya, S. G., Britto, J. D. J., Jose, M., and Das, S. J. (2022). Visible-light active zinc doped cobalt oxide (Zn-Co_3O_4) nanoparticles for photocatalytic and photochemical activity. *Mater. Today Proc.* 68, 269–275. doi:10.1016/j.matpr.2022.05.167

Selvakumar, G., and Palanivel, C. (2022). A study on synthesis, characterization and catalytic applications of MoO_3-ZnO nanocompositematerial. *Mater. Sci. Energy Technol.* 5, 36–44. doi:10.1016/j.mset.2021.11.005

Sudhaik, A., Raizada, P., Singh, P., Hosseini-Bandegharaei, A., Thakur, V. K., and Nguyen, V.-H. (2020). Highly effective degradation of imidacloprid by H2O2/fullerene decorated P-doped g-C_3N_4 photocatalyst. *J. Environ. Chem. Eng.* 8 (6), 104483. doi:10.1016/j.jece.2020.104483

Swaminathan, M., Muruganandham, M., and Sillanpaa, M. (2013). Advanced oxidation processes for wastewater treatment. *Hindawi* 2013, 1–3. doi:10.1155/2013/683682

Velempini, T., Prabakaran, E., and Pillay, K. (2021). Recent developments in the use of metal oxides for photocatalytic degradation of pharmaceutical pollutants in water—a review. *Mater. Today Chem.* 19, 100380. doi:10.1016/j.mtchem.2020.100380

Villaverde, J. J., López-Goti, C., Alcamí, M., Lamsabhi, A. M., Alonso-Prados, J. L., and Sandín-España, P. (2017). Quantum chemistry in environmental pesticide risk assessment. *Pest Manag. Sci.* 73 (11), 2199–2202. doi:10.1002/ps.4641

Wang, X., Zhang, J., Wang, R., Ren, Y., Jin, S., Wang, S., et al. (2023). Stable all-solid-state Z-scheme heterojunction Bi_2O_3-Co_3O_4@ C microsphere photocatalysts for recalcitrant pollutant degradation. *J. Alloys Compd.* 2023, 168915. doi:10.1016/j.jallcom.2023.168915

Xue, S., Wu, C., Pu, S., Hou, Y., Tong, T., Yang, G., et al. (2019). Direct Z-Scheme charge transfer in heterostructured MoO_3/g-C_3N_4 photocatalysts and the generation of active radicals in photocatalytic dye degradations. *Environ. Pollut.* 250, 338–345. doi:10.1016/j.envpol.2019.04.010

Yari, K., Seidmohammadi, A., Khazaei, M., Bhatnagar, A., and Leili, M. (2019). A comparative study for the removal of imidacloprid insecticide from water by chemicalless UVC, UVC/TiO_2 and UVC/ZnO processes. *J. Environ. Health Sci. Eng.* 17, 337–351. doi:10.1007/s40201-019-00352-3

Zangeneh, H., Zinatizadeh, A., Habibi, M., Akia, M., and Isa, M. H. (2015). Photocatalytic oxidation of organic dyes and pollutants in wastewater using different modified titanium dioxides: A comparative review. *J. Industrial Eng. Chem.* 26, 1–36. doi:10.1016/j.jiec.2014.10.043

Zhang, C., Li, F., Zhang, H., Wen, R., Yi, X., Yang, Y., et al. (2021). Crucial roles of 3D–MoO_2–PBC cocatalytic electrodes in the enhanced degradation of imidacloprid in heterogeneous electro–fenton system: Degradation mechanisms and toxicity attenuation. *J. Hazard. Mater.* 420, 126556. doi:10.1016/j.jhazmat.2021.126556

Zheng, X., Li, Y., Peng, H., Huang, Z., Wang, H., and Wen, J. (2021). Efficient solar-light photodegradation of tetracycline hydrochloride using $BiVO_4/MoO_3$ composites. *Colloids Surfaces A Physicochem. Eng. Aspects* 621, 126599. doi:10.1016/j.colsurfa.2021.126599